Available online at www.sciencedirect.com
ScienceDirect
Journal of Sound and Vibration 316 (2008) 198–210
JOURNAL OF SOUND AND VIBRATION
www.elsevier.com/locate/jsvi

Vibrations of axially moving viscoelastic plate with parabolically varying thickness

Zhou Yin-feng*, Wang Zhong-min

School of Sciences, Xi'an University of Technology, Xi'an 710048, China

Received 16 June 2007; received in revised form 10 December 2007; accepted 24 February 2008
Handling Editor: L.G. Tham
Available online 14 April 2008

Abstract

Based on the two-dimensional viscoelastic differential constitutive relation, the differential equation of motion of the axially moving viscoelastic rectangular plate constituted by the Kelvin–Voigt model with parabolically varying thickness in the y-direction is derived. The dimensionless complex frequencies of axially moving viscoelastic plate with different boundary conditions versus the dimensionless moving speed for various aspect ratio, thickness parameter and the dimensionless delay time are analyzed by the differential quadrature method. The effects of various parameters such as aspect ratio, thickness parameter, the dimensionless moving speed and the dimensionless delay time on the vibration characteristics of the axially moving viscoelastic rectangular plate with parabolically varying thickness are discussed.

1. Introduction

Varying thickness plates are widely used in aerospace structures in order to economize on the plate materials or lighten the plates. Therefore, it is of great importance to study vibration characteristics of plates with varying thickness. Compared to the large amount of research studies on rectangular plates with linearly varying thickness [1–4], the published works on parabolically varying thickness plates are limited [5,6]. Because the governing equation of the plate with parabolically varying thickness is four-order variable coefficients partial differential equation, it makes the computation of the natural frequencies more complicated than those of uniform-thickness plates. Differential quadrature method (DQM) as an efficient alternative numerical tool for structural analysis has been widely used for static and free vibration analysis of beams and plates. In application to such problems it was concluded that DQM procedures offer comparable accuracy with less computation with those of Rayleigh–Ritz method, finite difference and finite element methods (FEM).

Thus, the purposes of this paper are to discuss the transverse vibration of the axially moving viscoelastic rectangular thin plate constituted by the Kelvin–Voigt model with parabolically varying thickness in the y-

*Corresponding author.
E-mail address: yinfengzhou@163.com (Z. Yin-feng).

0022-460X/$ - see front matter © 2008 Elsevier Ltd. All rights reserved.
doi:10.1016/j.jsv.2008.02.040

direction by DQM, and to investigate the effects of the aspect ratio, thickness parameter, the dimensionless moving speed and the dimensionless delay time of the material on the dynamic behaviors and stability of the moving viscoelastic plate with parabolically varying thickness.

2. Governing equations

Fig. 1 shows a viscoelastic rectangular thin plate with parabolically varying thickness in the y-direction and moving with constant speed v in the x-direction. The plate has the length a in the x-direction, width b in the y-direction, thickness h_1 and h_2 on $y = b/2$ and $y = 0$, b, respectively. The thickness is assumed to vary in the y-direction according to the relation $h(y) = h_1\{h_2/h_1 + 4(1 - h_2/h_1)[y/b - (y/b)^2]\}$ as shown in Fig. 1. The density of the material is ρ.

Assuming elastic behavior in dilatation and the Kelvin–Voigt law for distortion, the constitutive equations are as follows [7]:

$$\begin{cases} s_{ij} = 2Ge_{ij} + 2\eta\dot{e}_{ij} \\ \sigma_{ii} = 3K\varepsilon_{ii} \end{cases} \tag{1}$$

where G is shear elastic modulus, K is bulk elastic modulus, and η is viscosity coefficient.

According to the thin plate theory and the constitutive equations of the viscoelastic material in Laplace domain [8], the differential equation of motion of axially moving viscoelastic rectangular plate with parabolically varying thickness constituted by the Kelvin–Voigt model in time domain is

$$\begin{aligned} &h^3(y)\left(A_3 + A_4\frac{\partial}{\partial t} + A_5\frac{\partial^2}{\partial t^2}\right)\nabla^4\overline{w} + 6h^2(y)\frac{\mathrm{d}h(y)}{\mathrm{d}y}\left(A_3 + A_4\frac{\partial}{\partial t} + A_5\frac{\partial^2}{\partial t^2}\right)\frac{\partial}{\partial y}\nabla^2\overline{w} \\ &+ 6h(y)\left(\frac{\mathrm{d}h(y)}{\mathrm{d}y}\right)^2\left[\left(A_6 + A_7\frac{\partial}{\partial t} - A_5\frac{\partial^2}{\partial t^2}\right)\left(\frac{\partial^2\bar{w}}{\partial x^2}\right)\left(A_3 + A_4\frac{\partial}{\partial t} + A_5\frac{\partial^2}{\partial t^2}\right)\left(\frac{\partial^2\bar{w}}{\partial y^2}\right)\right] \\ &- 12\rho h(y)\left(A_1 + A_2\frac{\partial}{\partial t}\right)\left(\frac{\partial^2\overline{w}}{\partial t^2} + 2v\frac{\partial^2\overline{w}}{\partial t\partial x} + v^2\frac{\partial^2\overline{w}}{\partial x^2}\right) = 0 \end{aligned} \tag{2}$$

where $\overline{w}(x, y, t)$ is deflection function of the plate, $A_1 = 3K + 4G$, $A_2 = 4\eta$, $A_3 = 2G(6K + 2G)$, $A_4 = 8G\eta + 12K\eta$, $A_5 = 4\eta^2$, $A_6 = 2G(3K - 2G)$, $A_7 = 6K\eta - 8G\eta$, $G = E/2(1 + \mu)$, $K = E/3(1 - 2\mu)$, μ is Poisson's ratio.

$$\nabla^4\bar{w} = \partial^4\overline{w}/\partial x^4 + 2(\partial^4\overline{w}/\partial x^2\partial y^2) + \partial^4\overline{w}/\partial y^4, \quad \nabla^2\overline{w} = \partial^2\overline{w}/\partial x^2 + \partial^2\overline{w}/\partial y^2.$$

It is convenient to introduce the dimensionless variables and parameters

$$\begin{aligned} &\xi = \frac{x}{a}, \quad \psi = \frac{y}{b}, \quad \overline{W} = \frac{\overline{w}}{h_1}, \quad \lambda = \frac{a}{b}, \quad \tau = \frac{h_1}{a^2}\sqrt{\frac{E}{12\rho(1-\mu^2)}}t, \\ &c = \frac{a}{h_1}\sqrt{\frac{12\rho(1-\mu^2)}{E}}v, \quad H = \frac{h_1}{a^2}\sqrt{\frac{E}{12\rho(1-\mu^2)}}\frac{\eta}{E} \end{aligned} \tag{3}$$

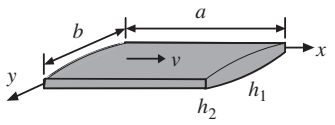

Fig. 1. Axially moving viscoelastic plate with parabolically varying thickness.

Substituting Eq. (3) into Eq. (2), the dimensionless differential equation of motion for the axially moving viscoelastic plate with parabolically varying thickness constituted by the Kelvin–Viogt model is written as

$$\begin{aligned}&\left[\frac{h_2}{h_1}+4\left(1-\frac{h_2}{h_1}\right)(\psi-\psi^2)\right]^2\left(1+a_1\frac{\partial}{\partial\tau}+a_2\frac{\partial^2}{\partial\tau^2}\right)\nabla^4\overline{W}+6\left[\frac{h_2}{h_1}+4\left(1-\frac{h_2}{h_1}\right)(\psi-\psi^2)\right]\\&\times 4\left(1-\frac{h_2}{h_1}\right)(1-2\psi)\left(1+a_1\frac{\partial}{\partial\tau}+a_2\frac{\partial^2}{\partial\tau^2}\right)\frac{\partial}{\partial\psi}\nabla^2\overline{W}+6\left[4\left(1-\frac{h_2}{h_1}\right)(1-2\psi)\right]^2\\&\times\left[\left(a_3+a_4\frac{\partial}{\partial\tau}-a_2\frac{\partial^2}{\partial\tau^2}\right)\frac{\partial^2\overline{W}}{\partial\xi^2}+\left(1+a_1\frac{\partial}{\partial\tau}+a_2\frac{\partial^2}{\partial\tau^2}\right)\frac{\partial^2\overline{W}}{\partial\psi^2}\right]+\left(1+a_5\frac{\partial}{\partial\tau}\right)\\&\times\left(\frac{\partial^2\overline{W}}{\partial\tau^2}+2c\frac{\partial^2\overline{W}}{\partial\xi\partial\tau}+c^2\frac{\partial^2\overline{W}}{\partial\xi^2}\right)=0\end{aligned}\tag{4}$$

where τ is dimensionless time, c is dimensionless axially moving speed, H is dimensionless delay time of material, $a_1=\frac{4}{3}(2-\mu)(1+\mu)$, $a_2=\frac{4}{3}(1-2\mu)(1+\mu)^2$, $a_3=\mu$, $a_4=\frac{2}{3}(1+\mu)(5\mu-1)$, $a_5=4(1-2\mu)(1+\mu)/3(1-\mu)$,

$$\nabla^4\overline{W}=\partial^4\overline{W}/\partial\xi^4+2\lambda^2(\partial^4\overline{W}/\partial\xi^2\partial\psi^2)+\lambda^4(\partial^4\overline{W}/\partial\psi^4),\quad \nabla^2\overline{W}=\partial^2\overline{W}/\partial\xi^2+\lambda^2(\partial^2\overline{W}/\partial\psi^2).$$

Let Eq. (4) has a solution of the form:

$$\overline{W}(\xi,\psi,\tau)=W(\xi,\psi)\,\mathrm{e}^{\mathrm{j}\omega\tau}\tag{5}$$

Then the dimensionless form of Eq. (4) becomes

$$\begin{aligned}&\left[\frac{h_2}{h_1}+4\left(1-\frac{h_2}{h_1}\right)(\psi-\psi^2)\right]^2D_1\nabla^4W+6\left[\frac{h_2}{h_1}+4\left(1-\frac{h_2}{h_1}\right)(\psi-\psi^2)\right]4\left(1-\frac{h_2}{h_1}\right)\\&\times(1-2\psi)\lambda^2D_1\frac{\partial}{\partial\psi}\nabla^2W+6\left[4\left(1-\frac{h_2}{h_1}\right)(1-2\psi)\right]^2\left(D_2\lambda^2\frac{\partial^2W}{\partial\xi^2}+D_1\lambda^4\frac{\partial^2W}{\partial\psi^2}\right)\\&+D_3\left(\mathrm{j}^2\omega^2W+2c\mathrm{j}\omega\frac{\partial W}{\partial\xi}+c^2\frac{\partial^2W}{\partial\xi^2}\right)=0\end{aligned}\tag{6}$$

where $\mathrm{j}=\sqrt{-1}$, ω is the dimensionless complex frequency of the transverse vibration of the viscoelastic plate. $D_1=1+a_1H\mathrm{j}\omega+a_2H^2\mathrm{j}^2\omega^2$, $D_2=a_3+a_4H\mathrm{j}\omega-a_2H^2\mathrm{j}^2\omega^2$, $D_3=1+a_5H\mathrm{j}\omega$,

$$\nabla^4W=\partial^4W/\partial\xi^4+2\lambda^2(\partial^4W/\partial\xi^2\partial\psi^2)+\lambda^4(\partial^4W/\partial\psi^4),\quad \nabla^2W=\partial^2W/\partial\xi^2+\lambda^2(\partial^2W/\partial\psi^2).$$

The boundary conditions of the plate with four edges simply supported are

$$\begin{cases}\xi=0,1: & W(\xi,\psi)=\dfrac{\partial^2W}{\partial\xi^2}=0\\ \psi=0,1: & W(\xi,\psi)=\dfrac{\partial^2W}{\partial\psi^2}=0\end{cases}\tag{7}$$

The boundary conditions of the plate with two opposite edges simply supported and other edges clamped are

$$\begin{cases}\xi=0,1: & W(\xi,\psi)=\dfrac{\partial W}{\partial\xi}=0\\ \psi=0,1: & W(\xi,\psi)=\dfrac{\partial^2W}{\partial\psi^2}=0\end{cases}\tag{8}$$

3. Differential quadrature analogs

The basic idea of the DQ method is to approximate the partial derivatives of a function with respect to a spatial variable at any discrete point as the weighted linear sum of the function values at all the discrete points

chosen in the solution domain of spatial variable [9]. Consider smooth function $f(x, y)$ in region $0 \leqslant x \leqslant a$, $0 \leqslant y \leqslant b$, the partial derivative of the rth order with respect to x of it at the point (x_i, y_i), the partial derivative of the sth order with respect to y, the mixed partial derivative of the sth order with respect to y and the rth order with respect to x are defined as follows, respectively [10]:

$$\frac{\partial^r f(x_i, y_j)}{\partial x^r} = \sum_{k=1}^{N} A_{ik}^{(r)} f(x_k, y_j) \quad (i = 1, 2, \ldots, N, \quad r = 1, 2, \ldots, N-1) \tag{9}$$

$$\frac{\partial^s f(x_i, y_j)}{\partial y^s} = \sum_{m=1}^{M} A_{jm}^{(s)} f(x_i, y_m) \quad (j = 1, 2, \ldots, M, \quad s = 1, 2, \ldots, N-1) \tag{10}$$

$$\frac{\partial^{r+s} f(x_i, y_j)}{\partial x^r \partial y^s} = \sum_{k=1}^{N} A_{ik}^{(r)} \sum_{m=1}^{M} A_{jm}^{(s)} f(x_i, y_m) \tag{11}$$

where N and M are the number of grid points in x and y-directions, respectively, $A_{ik}^{(r)}$and $A_{jm}^{(s)}$ are weight coefficients, and they are defined by

$$A_{ik}^{(1)} = \begin{cases} \prod\limits_{\substack{\mu=1 \\ \mu \neq i,k}}^{N} (x_i - x_\mu) \Big/ \prod\limits_{\substack{\mu=1 \\ \mu \neq k}}^{N} (x_k - x_\mu) & (i, k = 1, 2, \ldots, N, \quad k \neq i) \\ \sum\limits_{\substack{\mu=1 \\ \mu \neq i}}^{N} \dfrac{1}{x_i - x_\mu} & (i, k = 1, 2, \ldots, N, \quad k = i) \end{cases} \tag{12}$$

$$A_{jm}^{(1)} = \begin{cases} \prod\limits_{\substack{\mu=1 \\ \mu \neq j,m}}^{M} \left(y_j - y_\mu\right) \Big/ \prod\limits_{\substack{\mu=1 \\ \mu \neq m}}^{M} \left(y_m - y_\mu\right) & (j, m = 1, 2, \ldots, M, \quad m \neq j) \\ \sum\limits_{\substack{\mu=1 \\ \mu \neq j}}^{M} \dfrac{1}{y_j - y_\mu} & (j, m = 1, 2, \ldots, M, \quad m = j) \end{cases} \tag{13}$$

In the case of $r = 2, 3, \ldots, N-1, \quad s = 2, 3, \ldots, M-1$,

$$A_{ik}^{(r)} = \begin{cases} r\left(A_{ii}^{(r-1)} A_{ik}^{(1)} - \dfrac{A_{ik}^{(r-1)}}{x_i - x_k}\right) & (i, k = 1, 2, \ldots, N, \quad k \neq i) \\ -\sum\limits_{\substack{\mu=1 \\ \mu \neq i}}^{N} A_{i\mu}^{(r)} & (i = 1, 2, \ldots, N, \quad 1 \leqslant r \leqslant (N-1)) \end{cases} \tag{14}$$

$$A_{jm}^{(s)} = \begin{cases} s\left(A_{jj}^{(s-1)} A_{jm}^{(1)} - \dfrac{A_{jm}^{(s-1)}}{y_j - y_m}\right) & (j, m = 1, 2, \ldots, M, \quad m \neq j) \\ -\sum\limits_{\substack{\mu=1 \\ \mu \neq j}}^{M} A_{j\mu}^{(s)} & (j = 1, 2, \ldots, M, \quad 1 \leqslant s \leqslant (M-1)) \end{cases} \tag{15}$$

There are two key points in the successful application of the differential quadrature method, one is how to determine the weighting coefficients and the other is how to select the grid points. The natural and simplest choice of the grid points is equally spaced points in the direction of the coordinate axes of the computational domain. It was demonstrated that non-uniform grid points gives a better results with the same number of equally spaced grid points [11]. In this paper, we choose these set of grid points in terms of natural coordinate directions ξ and ψ for the plate with four edges simply supported and the plate with two opposite edges simply

supported and other edges clamped, respectively as

$$\begin{cases} \xi_1 = 0, \ \ \xi_N = 1, \ \ \xi_i = \dfrac{1}{2}\left[1 - \cos\left(\dfrac{2i-3}{2N-4}\pi\right)\right] & (i = 2, 3 \ldots, N-1) \\ \psi_1 = 0, \ \ \psi_N = 1, \ \ \psi_i = \dfrac{1}{2}\left[1 - \cos\left(\dfrac{2i-3}{2N-4}\pi\right)\right] & (i = 2, 3, \ldots, N-1) \end{cases} \tag{16}$$

$$\begin{cases} \xi_1 = 0, \ \ \xi_2 = \delta, \ \ \xi_{N-1} = 1-\delta, \ \ \xi_N = 1, \ \ \xi_i = \dfrac{1}{2}\left[1 - \cos\left(\dfrac{i-2}{N-3}\pi\right)\right] & (i = 3, 4, \ldots, N-2) \\ \psi_1 = 0, \ \ \psi_N = 1, \ \ \psi_i = \dfrac{1}{2}\left[1 - \cos\left(\dfrac{2i-3}{2N-4}\pi\right)\right] & (i = 2, 3, \ldots, N-1) \end{cases} \tag{17}$$

To formulate the eigenvalue equations, the governing differential equations with their associated boundary conditions are transformed into algebraic equations via DQM:

$$\begin{aligned} &\left[\frac{h_2}{h_1} + 4\left(1 - \frac{h_2}{h_1}\right)(\psi - \psi^2)\right]^2 \left(\sum_{k=1}^{N} A_{ik}^{(4)} W_{kj} + 2\lambda^2 \sum_{m=1}^{N} A_{jm}^{(2)} \sum_{k=1}^{N} A_{ik}^{(2)} W_{km} + \lambda^4 \sum_{k=1}^{N} A_{jk}^{(4)} W_{ik}\right) \\ &+ 6\left[\frac{h_2}{h_1} + 4\left(1 - \frac{h_2}{h_1}\right)(\psi - \psi^2)\right] 4\left(1 - \frac{h_2}{h_1}\right)(1 - 2\psi)\left(\lambda^2 \sum_{m=1}^{N} A_{jm}^{(1)} \sum_{k=1}^{N} A_{ik}^{(2)} W_{km} + \lambda^4 \sum_{k=1}^{N} A_{jk}^{(3)} W_{ik}\right) \\ &+ 6\left[4\left(1 - \frac{h_2}{h_1}\right)(1 - 2\psi)\right]^2 \left(a_3\lambda^2 \sum_{k=1}^{N} A_{ik}^{(2)} W_{kj} + \lambda^4 \sum_{k=1}^{N} A_{jk}^{(2)} W_{ik}\right) + c^2 \sum_{k=1}^{N} A_{ik}^{(2)} W_{kj} \\ &+ \left\{\left[\frac{h_2}{h_1} + 4\left(1 - \frac{h_2}{h_1}\right)(\psi - \psi^2)\right]^2 a_1 \left(\sum_{k=1}^{N} A_{ik}^{(4)} W_{kj} + 2\lambda^2 \sum_{m=1}^{N} A_{jm}^{(2)} \sum_{k=1}^{N} A_{ik}^{(2)} W_{km} + \lambda^4 \sum_{k=1}^{N} A_{jk}^{(4)} W_{ik}\right) \mathrm{Hj} \right. \\ &+ 6\left[\frac{h_2}{h_1} + 4\left(1 - \frac{h_2}{h_1}\right)(\psi - \psi^2)\right] 4\left(1 - \frac{h_2}{h_1}\right)(1 - 2\psi) a_1 \left(\lambda^2 \sum_{m=1}^{N} A_{jm}^{(1)} \sum_{k=1}^{N} A_{ik}^{(2)} W_{km} + \lambda^4 \sum_{k=1}^{N} A_{jk}^{(3)} W_{ik}\right) \mathrm{Hj} \\ &+ 6\left[4\left(1 - \frac{h_2}{h_1}\right)(1 - 2\psi)\right]^2 \left(a_4\lambda^2 \sum_{k=1}^{N} A_{ik}^{(2)} W_{kj} + a_1\lambda^4 \sum_{k=1}^{N} A_{jk}^{(2)} W_{ik}\right) \mathrm{Hj} + 2c\mathrm{j} \sum_{k=1}^{N} A_{ik}^{(1)} W_{kj} \\ &\left. a_5 c^2 \sum_{k=1}^{N} A_{ik}^{(2)} W_{kj} \mathrm{Hj}\right\} \omega + \left\{\left[\frac{h_2}{h_1} + 4\left(1 - \frac{h_2}{h_1}\right)(\psi - \psi^2)\right]^2 a_2 \left(\sum_{k=1}^{N} A_{ik}^{(4)} W_{kj} + 2\lambda^2 \sum_{m=1}^{N} A_{jm}^{(2)} \sum_{k=1}^{N} A_{ik}^{(2)} W_{km} \right.\right. \\ &+ \lambda^4 \sum_{k=1}^{N} A_{jk}^{(4)} W_{ik}\Big) H^2 \mathrm{j}^2 + 6\left[\frac{h_2}{h_1} + 4\left(1 - \frac{h_2}{h_1}\right)(\psi - \psi^2)\right] 4\left(1 - \frac{h_2}{h_1}\right)(1 - 2\psi) a_2 \left(\lambda^2 \sum_{m=1}^{N} A_{jm}^{(1)} \sum_{k=1}^{N} A_{ik}^{(2)} W_{km}\right. \\ &+ \lambda^4 \sum_{k=1}^{N} A_{jk}^{(3)} W_{ik}) H^2 \mathrm{j}^2 - W + 6\left[4\left(1 - \frac{h_2}{h_1}\right)(1 - 2\psi)\right]^2 \left(a_2\lambda^2 \sum_{k=1}^{N} A_{ik}^{(2)} W_{kj} - a_2\lambda^4 \sum_{k=1}^{N} A_{jk}^{(2)} W_{ik}\right) H^2 \\ &\left.\left. + 2a_5 c H\mathrm{j} \sum_{k=1}^{N} A_{ik}^{(1)} W_{kj}\right\} \omega^2 - a_5 H\mathrm{j} W \omega^3 = 0 \end{aligned} \tag{18}$$

$$\begin{cases} W_{1j} = W_{Nj} = W_{i1} = W_{iN} = 0 & i, j = 1, 2, \ldots, N \\ \sum\limits_{k=1}^{N} A_{ik}^{(2)} W_{kj} = 0 & i = 1, N, \quad j = 1, 2, \ldots, N \\ \sum\limits_{k=1}^{N} A_{jk}^{(2)} W_{ik} = 0 & j = 1, N, \quad i = 1, 2, \ldots, N \end{cases} \tag{19}$$

$$\begin{cases} W_{1j} = W_{Nj} = W_{i1} = W_{iN} = 0 & i,j = 1,2,\ldots,N \\ \sum_{k=1}^{N} A_{ik}^{(1)} W_{kj} = 0 & i = 2, N-1, \quad j = 2,3,\ldots,N-2 \\ \sum_{k=1}^{N} A_{jk}^{(2)} W_{ik} = 0 & j = 1, N, \quad i = 1,2,\ldots,N \end{cases} \tag{20}$$

Eq. (18) and boundary conditions (19) or (20) can be written into matrix form

$$(\omega^3[Q] + \omega^2[R] + \omega[G] + [K])\{W_{kj}\} = \{0\} \tag{21}$$

where the matrices $[Q],[R],[G],[K]$ involve parameters such as dimensionless delay time H, dimensionless axially moving speed c, thickness parameter and aspect ratio of the plate. Eq. (21) is a generalized eigenvalue problem, it can be solved by using standard eigenvalue routine for a complex general matrix, then natural frequencies as well as mode shapes can be obtained. In this work, Matlab software has been employed for the solution procedure.

4. Numerical examples and discussion

If $H = 0$, $c = 0$, thickness parameter $h_2/h_1 = 1$, Eq. (6) is reduced to transverse free vibration of uniform-thickness elastic plate. In order to verify the DQM, the first three-order natural frequencies of the transverse free vibration of elastic plate with two different boundary conditions are calculated firstly, the results in this paper are in good agreement with those in Ref. [12], which can be seen from Table 1.

Now, the dynamic behaviors and stability of the axially moving viscoelastic rectangular plate constituted by the Kelvin–Voigt model with parabolically varying thickness are calculated and analyzed.

4.1. The plate with four edges simply supported

Fig. 2 shows the variation of the first three-order dimensionless complex frequencies of the plate with dimensionless axially moving speed for $\lambda = 1$, $h_2/h_1 = 1$, $H = 10^{-5}$. It can be seen that, when dimensionless moving speed $c = 0$, dimensionless complex frequency ω is a real number. With the increase of axially moving speed, the real part of ω decreases, while its imaginary part remains zero. When moving speed increases to critical value $c = 6.31$, the real part of ω in the first mode becomes zero, subsequently, $\mathrm{Re}(\omega) = 0$ but $\mathrm{Im}(\omega) > 0$ and $\mathrm{Im}(\omega) < 0$ occur, this shows that the plate behaves divergent instability. When moving speed further increases to $c = 7.81$, the plate regains stability in the first-order mode. After the plate gains restability, in the case of $c = 8.31$, $\mathrm{Re}(\omega) \neq 0$ and the imaginary part of ω has two branches with positive and negative value, it indicates that the first-order mode couples the second-order mode, that is the plate undergoes coupled-mode flutter.

Fig. 3 gives the variation of the first three-order dimensionless complex frequencies of the plate with dimensionless axially moving speed for $\lambda = 1$, $h_2/h_1 = 1$, $H = 10^{-3}$. In comparison with Fig. 2, because of the increase of the dimensionless delay time, the imaginary part of the dimensionless complex frequency ω does not remain zero, but are positive value, and it increase with the increase of mode order. The increase of the dimensionless delay time does not have effect on the critical divergence speed of the first-order mode, but the first-order mode does not couple the second-order mode.

Table 1
The first three order natural frequencies of the transverse free vibration of the elastic plate with different boundary conditions ($c = 0$)

	Aspect ratio λ	0.5			1		
The solution in this paper	SSSS	12.3370	19.7401	31.8919	19.7392	49.3519	78.9647
	CSCS	23.8184	28.9567	38.9379	28.9559	54.7467	69.3392
Exact solution [12]	SSSS	12.33	19.73	32.07	19.73	49.35	78.96
	CSCS	23.82	28.95	39.09	28.95	54.74	69.33

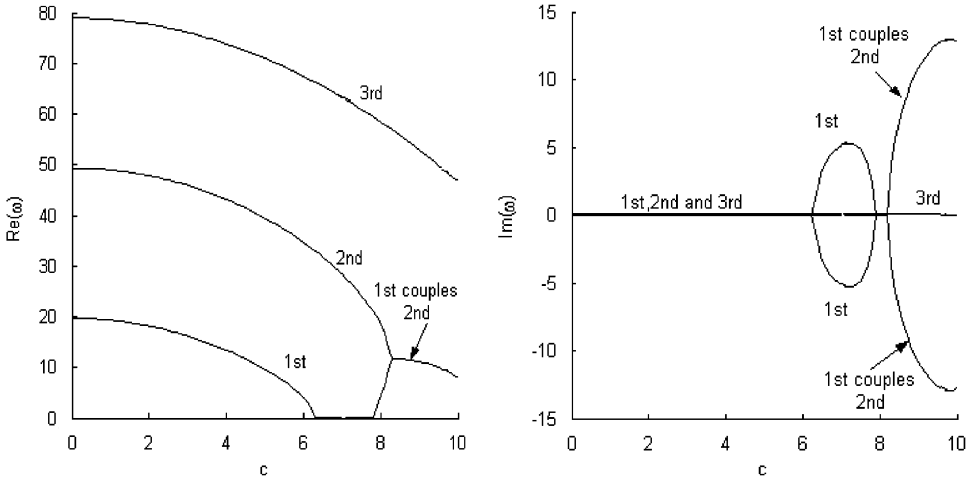

Fig. 2. Dimensionless complex frequency versus the dimensionless axially moving speed for SSSS plate for $H = 10^{-5}$, $\lambda = 1$, $h_2/h_1 = 1$.

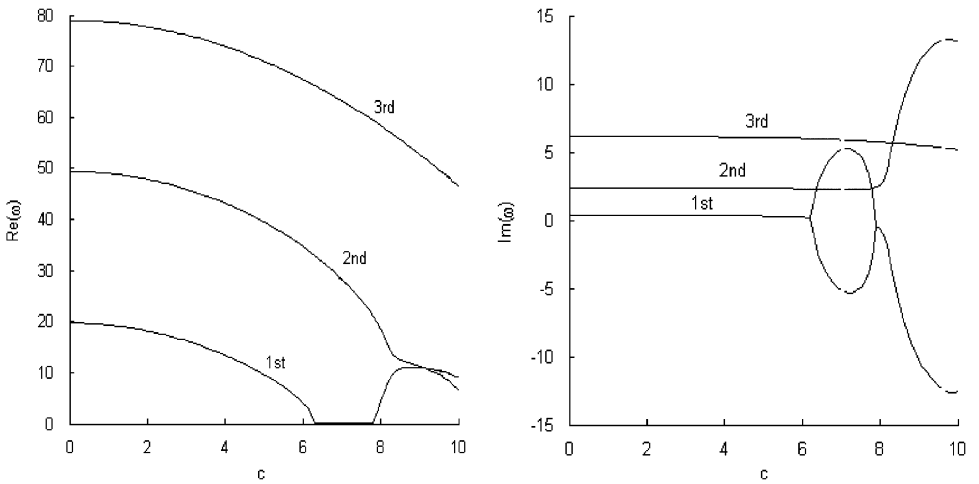

Fig. 3. Dimensionless complex frequency versus the dimensionless axially moving speed for SSSS plate for $H = 10^{-3}$, $\lambda = 1$, $h_2/h_1 = 1$.

Fig. 4 shows the variation of the first three-order dimensionless complex frequencies of the plate with dimensionless axially moving speed for $\lambda = 1$, $h_2/h_1 = 0.5$, $H = 10^{-5}$. By contrast with Fig. 2, when dimensionless moving speed $c = 0$, dimensionless complex frequency ω is a complex number and the real part of it decreases evidently in comparison with the case of $h_2/h_1 = 1$. With the increase of axially moving speed, the real part of ω decreases, and its imaginary part remains a positive number. The critical divergence speed of the first-order mode and the critical speed of the first-order mode coupling the second-order mode decrease.

Fig. 5 gives the variation of the first three-order dimensionless complex frequencies of the plate with dimensionless axially moving speed for $H = 10^{-3}$, $\lambda = 1$, $h_2/h_1 = 0.5$. In comparison with Fig. 4, the increase of the dimensionless delay time does not have effect on the critical divergence speed of the first-order mode, but the plate does not undergo coupled-mode flutter.

Fig. 6 shows the variation of the first three-order dimensionless complex frequencies of the plate with dimensionless axially moving speed for $H = 10^{-5}$, $\lambda = 0.5$, $h_2/h_1 = 1$. By contrast with Fig. 2, when dimensionless moving speed $c = 0$, dimensionless complex frequency ω is also a real number, but it decreases evidently in comparison with the case of $\lambda = 1$. With the increase of axially moving speed, the real part of ω decreases, and its imaginary part remains zero too. The critical divergence speed of the first-order mode reduces to $c = 4$, subsequently, the plate behaves divergent instability in second-order mode at the speed

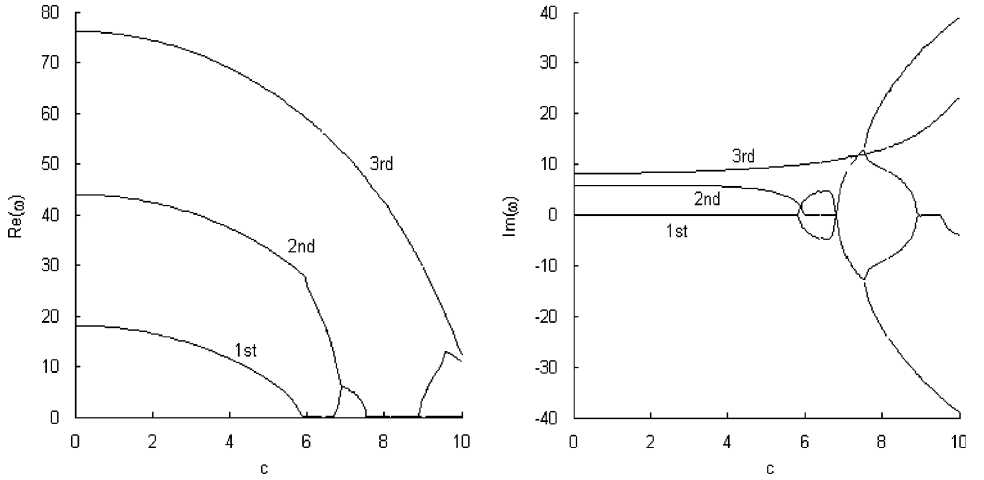

Fig. 4. Dimensionless complex frequency versus the dimensionless axially moving speed for SSSS plate for $H = 10^{-5}$, $\lambda = 1$, $h_2/h_1 = 0.5$.

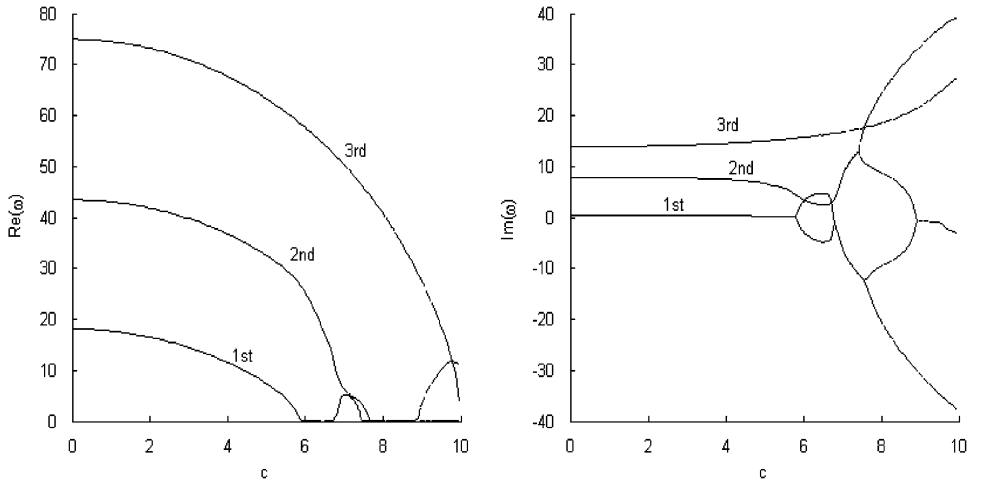

Fig. 5. Dimensionless complex frequency versus the dimensionless axially moving speed for SSSS plate for $H = 10^{-3}$, $\lambda = 1$, $h_2/h_1 = 0.5$.

$c = 6.31$. The critical speed of the plate undergoing coupled-mode flutter decrease to $c = 6.96$, and the modes in which the plate undergoes coupled-mode flutter is different from Fig. 2. When the moving speed increases to $c = 7.85$, the second-order mode regains stability.

Fig. 7 gives the variation of the first three-order dimensionless complex frequencies of the plate with dimensionless axially moving speed for $\lambda = 0.5$, $h_2/h_1 = 1$, $H = 10^{-3}$. In comparison with Fig. 4, because of the increase of the dimensionless delay time, the imaginary part of the dimensionless complex frequency ω becomes a positive value, and increase with the increase of mode order. The first-order mode does not couple the third-order mode.

4.2. The plate with two opposite edges simply supported and other two edges clamped

Figs. 8 and 9 gives the variation of the first three-order dimensionless complex frequencies of the plate with dimensionless axially moving speed for the same aspect ratio $\lambda = 1$, thickness parameter $h_2/h_1 = 1$, and different dimensionless delay time $H = 10^{-5}$, 10^{-3}. In the case of $H = 10^{-5}$, the first-order mode behaves divergent instability when dimensionless moving speed $c = 8.21$, after then, the plate regains stability at the moving speed $c = 10.31$. When the moving speed increases to $c = 11.09$, the first mode couple the third mode.

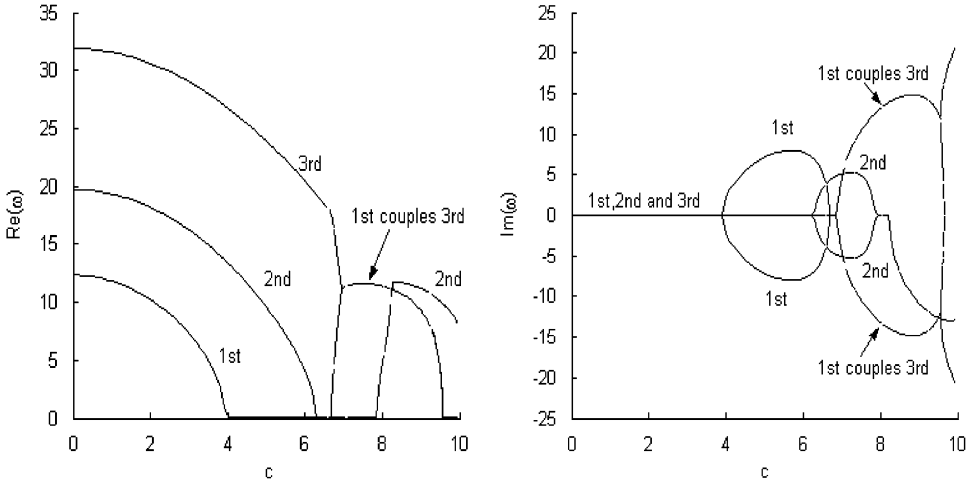

Fig. 6. Dimensionless complex frequency versus the dimensionless axially moving speed for SSSS plate for $H = 10^{-5}$, $\lambda = 0.5$, $h_2/h_1 = 1$.

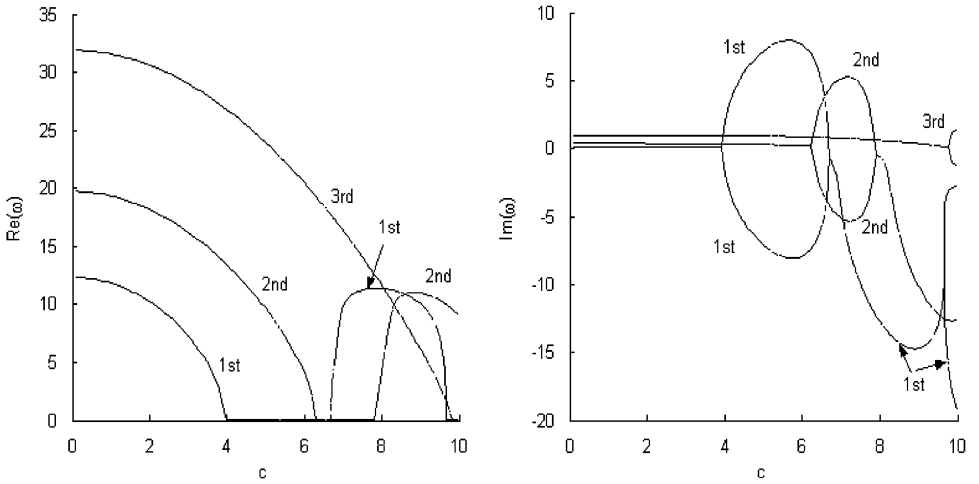

Fig. 7. Dimensionless complex frequency versus the dimensionless axially moving speed for SSSS plate for $H = 10^{-3}$, $\lambda = 0.5$, $h_2/h_1 = 1$.

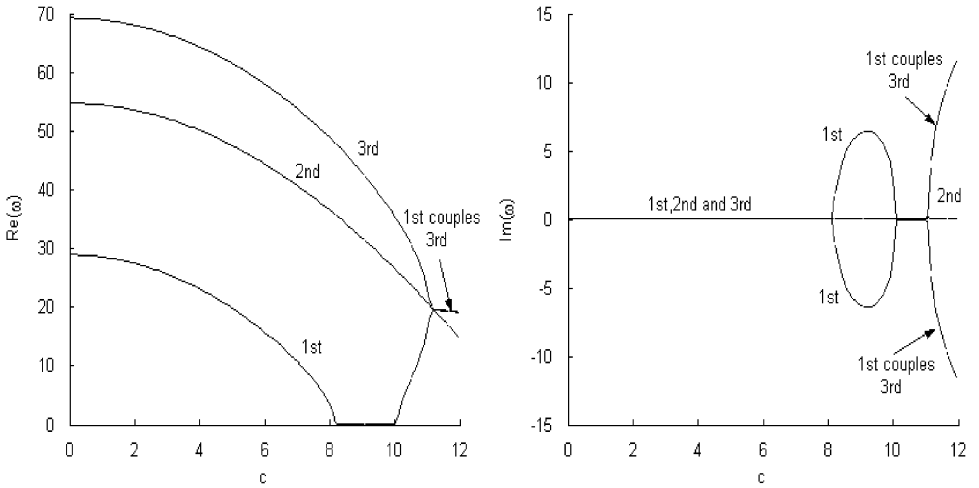

Fig. 8. Dimensionless complex frequency versus the dimensionless axially moving speed for CSCS plate for $H = 10^{-5}$, $\lambda = 1$, $h_2/h_1 = 1$.

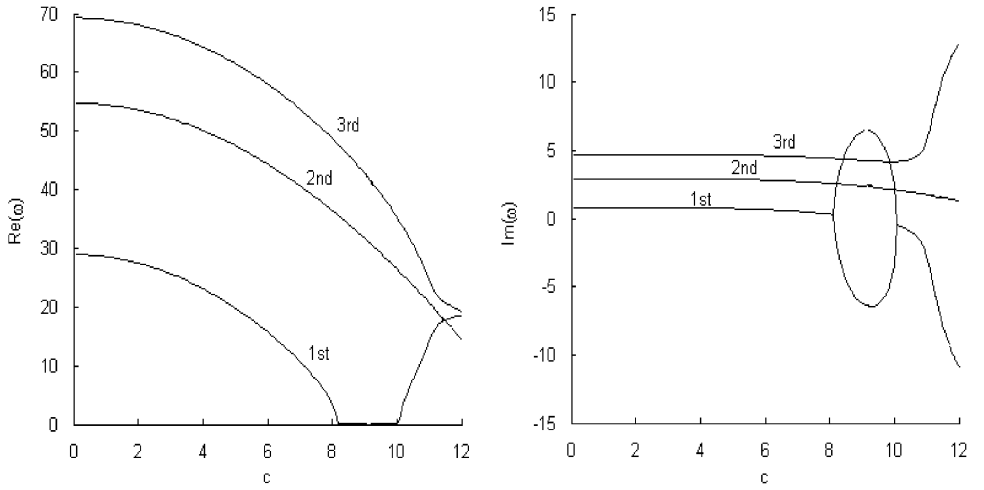

Fig. 9. Dimensionless complex frequency versus the dimensionless axially moving speed for CSCS plate $H = 10^{-5}$, $\lambda = 1$, $h_2/h_1 = 1$.

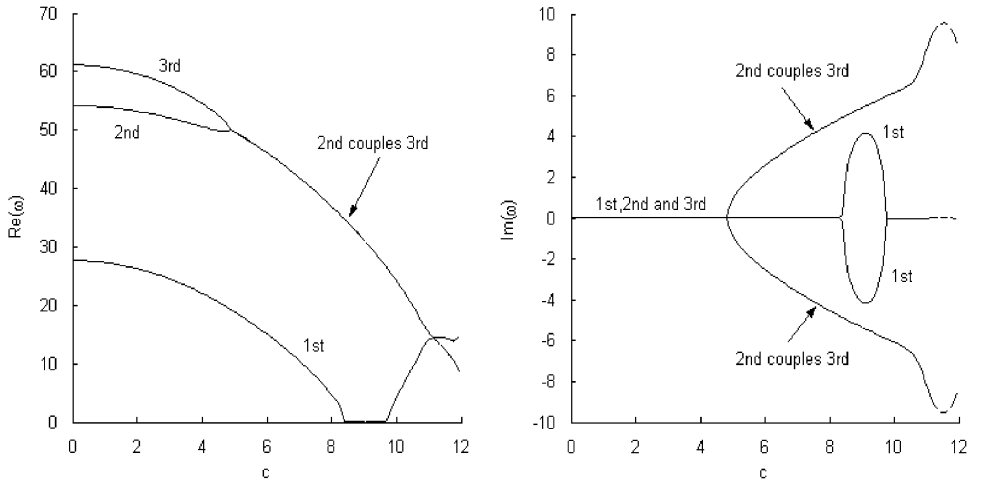

Fig. 10. Dimensionless complex frequency versus the dimensionless axially moving speed for CSCS plate $H = 10^{-5}$, $\lambda = 1$, $h_2/h_1 = 0.5$.

In the case of $H = 10^{-3}$, the increase of delay time does not have effect on the critical divergence speed of the first mode, but the imaginary parts of the complex frequencies change from zero to positive values, and the imaginary parts of the dimensionless complex frequencies of the first three modes increase with the increase of the modes order. The first mode and the third mode do not undergo coupled-mode flutter.

Figs. 10 and 11 gives the variation of the first three-order dimensionless complex frequencies of the plate with dimensionless axially moving speed for the same aspect ratio $\lambda = 1$, thickness parameter $h_2/h_1 = 0.5$, and different dimensionless delay time $H = 10^{-5}$, 10^{-3}. It is found that the second mode does not couples the third mode because of the increase of delay time, but the critical divergence speed of the first mode remains invariable. By contrast with Figs. 8 and 9, it indicates that the real parts of the complex frequencies decrease because of the decrease of thickness parameter, but the critical divergence speed of the first-order mode increases, and the modes in which the plate undergoes coupled-mode flutter change. Because of the decrease of thickness ratio, the plate undergoes coupled-mode flutter firstly, then it behaves divergent instability in first order.

Figs. 12 and 13 give the variation of the first three-order dimensionless complex frequencies of the plate with dimensionless axially moving speed for the same aspect ratio $\lambda = 0.5$, thickness parameter $h_2/h_1 = 1$, and

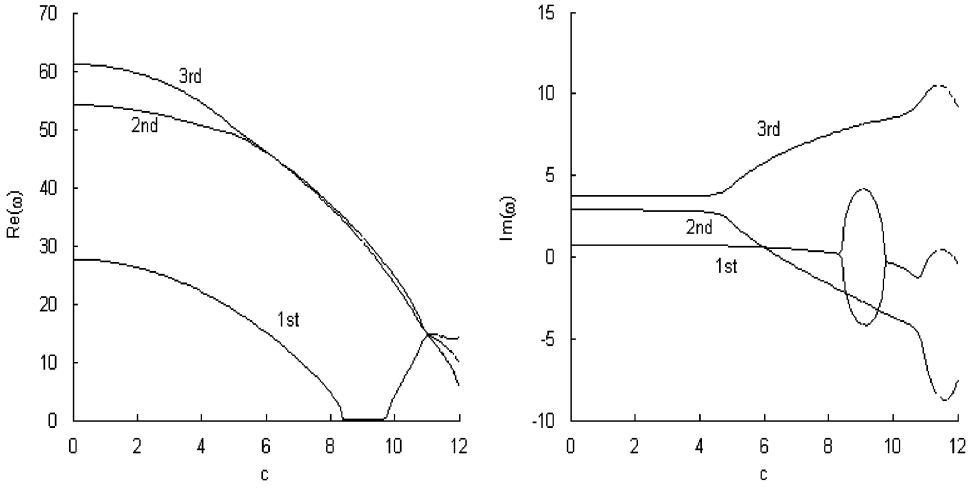

Fig. 11. Dimensionless complex frequency versus the dimensionless axially moving speed for CSCS plate $H = 10^{-3}$, $\lambda = 1$, $h_2/h_1 = 0.5$.

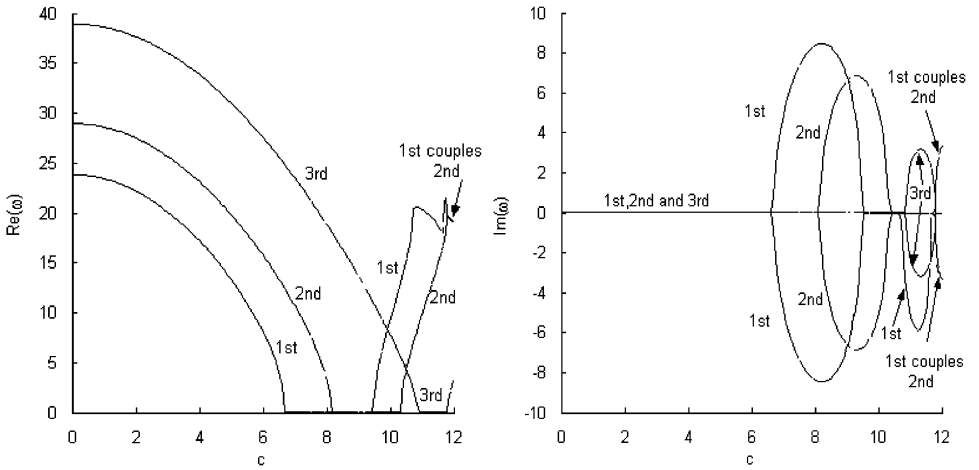

Fig. 12. Dimensionless complex frequency versus the dimensionless axially moving speed for CSCS plate $H = 10^{-5}$, $\lambda = 0.5$, $h_2/h_1 = 1$.

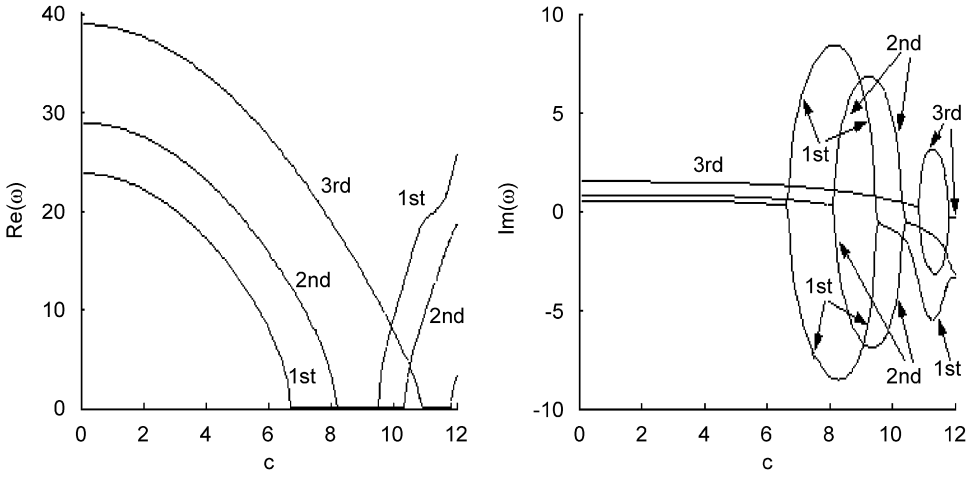

Fig. 13. Dimensionless complex frequency versus the dimensionless axially moving speed for CSCS plate $H = 10^{-3}$, $\lambda = 0.5$, $h_2/h_1 = 1$.

different dimensionless delay time $H = 10^{-5}, 10^{-3}$. As can be seen that the increase of delay time does not have effect on the critical divergence speeds of various modes, but the first mode does not couple the second mode. And because of the increase of delay time, the imaginary parts of the complex frequencies become positive values. By contrast with Figs. 8 and 9, respectively, it is obtained that the real parts of the first three dimensionless complex frequencies decrease with the decrease of aspect ratio, and the critical divergence speeds of various modes decrease too.

5. Conclusions

A DQ procedure for vibration analysis of axially moving viscoelastic plate with parabolically varying thickness was developed, the completeness of the present DQM was demonstrated for plates under different boundary conditions as well as the thickness variation. Dimensionless complex frequency versus the dimensionless axially moving speed are plotted for different boundary conditions and the effects of dimensionless delay time H, aspect ratio λ and thickness ratio h_2/h_1 on vibrations of axially moving viscoelastic rectangular plate constituted by the Kelvin–Voigt model with parabolically varying thickness are analyzed. The conclusions can be summarized as follows:

(1) For the SSSS plate and the CSCS plate, when other parameters are invariable, the increase of delay time (10^{-5}–10^{-3}) does not alter critical divergence speeds in various modes, but the plate does not undergo coupled-mode flutter, the imaginary parts of the first three complex frequencies don't remain zero, but are positive numbers, and increase with the increase of the modes.

(2) For the SSSS plate, when other parameters are invariable, with the decrease of thickness ratio h_2/h_1, the real parts of the first three complex frequencies decrease in the case of $c = 0$, and the critical divergence speeds of various modes decrease too, but the decrease of thickness ratio does not alter the modes that the plate undergo the coupled-mode flutter. With the decrease of aspect ratio, the real parts of the first three complex frequencies decrease evidently in the case of $c = 0$, and the critical divergence speeds in the first mode and the second mode decrease too, the modes that the plate undergoes coupled-mode flutter vary because of the decrease of aspect ratio.

(3) For the CSCS plate, when other parameters keep constants, with the decrease of thickness ratio h_2/h_1, the real parts of the first three complex frequencies decrease in the case of $c = 0$, but the critical divergence speeds of various modes increase, at the same time, the modes that the plate undergo the coupled-mode flutter change. With the decrease of aspect ratio, the real parts of the first three complex frequencies decrease evidently in the case of $c = 0$, and the critical divergence speeds in the first mode and the second mode decrease too, at the same time, the modes that the plate undergo coupled-mode flutter vary with the decrease of aspect ratio.

References

[1] G. Aksu, S.A. Al-Kaabi, Free vibration analysis of Mindlin plates with linearly varying thickness, *Journal of Sound and Vibration* 119 (1987) 189–205.
[2] T. Mizusawa, Vibration of rectangular Mindlin plates with tapered thickness by the spline strip method, *Computers and Structures* 46 (1993) 451–463.
[3] T. Sakiyama, M. Huang, Free vibration analysis of rectangular plates with variable thickness, *Journal of Sound and Vibration* 216 (1998) 379–397.
[4] T. Mizusawa, Y. Kondo, Application of the spline element method to analyze vibration of skew Mindlin plates with varying thickness in one direction, *Journal of Sound and Vibration* 241 (2001) 485–501.
[5] S.A. Al-Kaabi, G. Aksu, Free vibration analysis of Mindlin plates with parabolically varying thickness, *Computers and Structures* 34 (1990) 395–399.
[6] M. Ashraf, Zenkour, An exact solution for the bending of thin rectangular plates with uniform, linear and quadratic thickness variations, *International Journal of Mechanical Sciences* 45 (2003) 295–315.
[7] T.Q. Yang, *Viscoelasticity Theory and Applications*, Science Press, Beijing, 2004.
[8] W. Flügge, *Viscoelasticity*, second ed., Springer, Berlin, 1975.
[9] T.M. Teo, K.M. Liew, A differential quadrature procedure for three-dimensional buckling analysis of rectangular plates, *International Journal of Solids and Structures* 36 (1999) 1149–1168.

[10] A.S.J. Al-Saifl, Zh.Y. Zhu, Upwind local differential quadrature method for solving coupled viscous flow and heat transfer equations, *Applied Mathematics and Mechanics* 25 (10) (2004) 1034–1041.
[11] C.W. Bert, M. Malik, Differential quadrature method in computational mechanics: a review, *Applied Mechanic Review* 49 (1996) 1–27.
[12] D.J. Gorman, *Free Vibration Analysis of Rectangular Plates*, Elsevier, North Holland, 1982.